

Critical behavior near the metal-insulator transition in the one-dimensional extended Hubbard model at quarter filling

K. Sano

Department of Physics Engineering, Mie University, Tsu, Mie 514-8507, Japan

Y. Ōno

Department of Physics, Niigata University, Ikarashi, Niigata 950-2181, Japan

(December 20, 2006)

We examine the critical behavior near the metal-insulator transition (MIT) in the one-dimensional extended Hubbard model with the on-site and the nearest-neighbor interactions U and V at quarter filling using a combined method of the numerical diagonalization and the renormalization group (RG). The Luttinger-liquid parameter K_ρ is calculated with the exact diagonalization for finite size systems and is substituted into the RG equation as an initial condition to obtain K_ρ in the infinite size system. This approach also yields the charge gap Δ in the insulating state near the MIT. The results agree very well with the available exact results for $U = \infty$ even in the critical regime of the MIT where the characteristic energy becomes exponentially small and the usual finite size scaling is not applicable. When the system approaches the MIT critical point $V \rightarrow V_c$ for a fixed U , K_ρ and Δ behave as $|\ln \Delta|^{-2} = c_\Delta(V/V_c - 1)$ and $(K_\rho - \frac{1}{4})^2 = c_K(1 - V/V_c)$, where the critical value V_c and the coefficients c_Δ and c_K are functions of U . These critical properties, which are known to be exact for $U = \infty$, are observed also for finite U case. We also observe the same critical behavior in the limit of the MIT critical point $U \rightarrow U_c$ when U is varied for a fixed V .

PACS: 71.10Fd, 71.27.+a, 71.30.+h

I. INTRODUCTION

A number of theoretical studies have been made on the one-dimensional (1D) extended Hubbard model with the on-site interaction U and the nearest-neighbor interaction V as a simple model for quasi-1D materials¹⁻⁴. It has been reported that this model shows a rich phase diagram including the metal-insulator transition (MIT), the phase separation, the spin-gapped phase and the superconducting (SC) phase⁵⁻⁷. In particular, the MIT at quarter-filling has attracted much interest as it takes place for finite values of U and V in contrast to the MIT at half-filling where the system is insulating except for $U = 0$. Therefore, the MIT at quarter-filling is important as a typical example of the quantum phase transition caused by the electron correlation, and have been extensively studied by many authors⁷⁻¹³. However, the critical properties of the MIT have not received so much attention as it is more difficult to investigate the system in the limit of the MIT where the characteristic energy becomes exponentially small. In this paper, we wish to study the critical behavior near the MIT which is a typical example of the quantum critical phenomena caused by the electron correlation.

The extended Hubbard model is given by the following Hamiltonian

$$H = -t \sum_{i,\sigma} (c_{i\sigma}^\dagger c_{i+1\sigma} + h.c.) + U \sum_i n_{i\uparrow} n_{i\downarrow} + V \sum_{i,\sigma\sigma'} n_{i\sigma} n_{i+1\sigma'}, \quad (1)$$

where $c_{i\sigma}^\dagger$ stands for the creation operator of an electron with spin σ at site i and $n_{i\sigma} = c_{i\sigma}^\dagger c_{i\sigma}$. t represents the transfer energy between the nearest-neighbor sites and is set to be unity ($t=1$) in the present study. It is well known that this Hamiltonian (1) can be mapped on an XXZ quantum spin Hamiltonian in the limit $U \rightarrow \infty$. The term of the nearest-neighbor interaction V corresponds to the Z -component of the antiferromagnetic coupling and the transfer energy t does the X -component. When the Z -component is larger than the X -component, the system has a "Ising"-like symmetry and an excitation gap exists. For the Hubbard model, this corresponds to the case with $V > 2t$ where the charge gap is exactly obtained¹⁴. On the other hand, in the case with "XY"-like symmetry ($V < 2t$), the system is metallic and the Luttinger-liquid parameter K_ρ is exactly given by $\cos(\frac{\pi}{4K_\rho}) = -V/2$ ¹⁵.

In the finite U case, exact results have not been obtained except for $V = 0$. In this case, the weak coupling renormalization group method (known as g -ology) and the exact (numerical) diagonalization (ED) method have been applied. The g -ology yields the phase diagram of the 1D extended Hubbard model analytically, but quantitative validity is guaranteed only in the weak coupling regime^{1,2,12,13}. On the other hand, the numerical approach is a useful method to examine properties of the model in the strong coupling regime⁴⁻¹¹. In particular, the numerical diagonalization of a finite-size system has supplied us with reliable and important information⁵⁻¹⁰.

However, it is difficult for purely numerical approaches to investigate the critical behavior near the MIT where the characteristic energy scale of the system becomes ex-

ponentially small. To overcome this difficulty, we have recently proposed a combined approach of the ED and the RG methods.^{9,10} This approach enables us to obtain accurate results of the Luttinger-liquid parameter K_ρ and the charge gap Δ near the MIT beyond the usual finite size scaling for the ED method. The obtained results of K_ρ and Δ have been compared with the available exact results for $U = \infty$ and found to be in good agreement¹⁰. The phase diagram of the MIT at quarter-filling together with the contour map of the charge gap Δ has been obtained on the U - V plane¹⁰. However, the critical behavior near the MIT was not discussed in the previous work. Here we extensively apply this approach to the critical regime of the MIT to elucidate the critical behavior of K_ρ and Δ in the limit of the MIT.

II. LUTTINGER LIQUID AND RG METHOD

First, we briefly discuss a general argument for 1D-electron systems based on the bosonization theory¹⁻³. According to this theory, the effective Hamiltonian can be separated into the charge and spin parts. So, we turn our attention to only the charge part and do not consider the spin part in this work. In the low energy limit, the effective Hamiltonian of the charge part is given by

$$H_\rho = \frac{v_\rho}{2\pi} \int_0^L dx [K_\rho (\partial_x \theta_\rho)^2 + K_\rho^{-1} (\partial_x \phi_\rho)^2] + \frac{2g_{3\perp}}{(2\pi\alpha)^2} \int_0^L dx \cos[\sqrt{8}\phi_\rho(x)] \quad (2)$$

where v_ρ and K_ρ are the charge velocity and the coupling parameter, respectively. The operator ϕ_ρ and the dual operator θ_ρ represent the phase fields of the charge part. $g_{3\perp}$ denotes the amplitude of the umklapp scattering and α is a short-distance cutoff.

In the Luttinger liquid theory, some relations have been established as universal relations in one-dimensional models.³ In the model which is isotropic in spin space, the critical exponents of various types of correlation functions are determined by a single parameter K_ρ . It is predicted that the SC correlation is dominant for $K_\rho > 1$ (the correlation function decays as $\sim r^{-(1+\frac{1}{K_\rho})}$), whereas the CDW or SDW correlations are dominant for $K_\rho < 1$ (the correlation functions decay as $\sim r^{-(1+K_\rho)}$) in the Tomonaga-Luttinger liquid³. The critical exponent K_ρ is related to the charge susceptibility χ_c and the Drude weight D by

$$K_\rho = \frac{1}{2}(\pi\chi_c D)^{1/2}, \quad (3)$$

with $D = \frac{\pi}{N_a} \frac{\partial^2 E_0(\phi)}{\partial \phi^2}$, where $E_0(\phi)$ is the total energy of the ground state as a function of a magnetic flux $N_a\phi$ and N_a is the system size³. Here, the magnetic flux is imposed by introducing the following gauge transformation: $c_{m\sigma}^\dagger \rightarrow e^{im\phi/N_a} c_{m\sigma}^\dagger$ for an arbitrary site m .

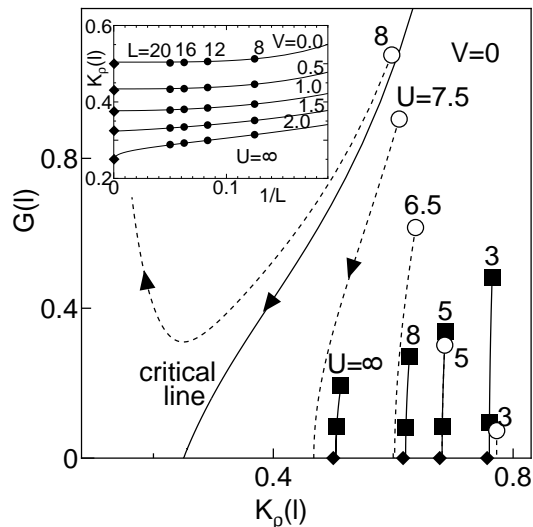


FIG. 1. The RG flow obtained from the numerical initial condition (solid lines) and that from the analytical one (broken lines) for various U at $V = 0$. The filled squares are the numerical initial conditions with $L_1 = 8$ and $L_2 = 12$, and the open circles are the analytical ones. The filled diamonds on the K_ρ axis are the exact results for $U = 3, 5, 8$ and ∞ . Inset shows the RG flow of $K_\rho(\ell)$ (solid lines), the numerical result of $K_\rho(\ell)$ (filled circles) and the exact result (filled diamonds) for various V at $U = \infty$.

When the charge gap vanishes in the thermodynamic limit, the uniform charge susceptibility χ_c is obtained from

$$\chi_c = \frac{4/N_a}{E_0(N_e + 2, N_a) + E_0(N_e - 2, N_a) - 2E_0(N_e, N_a)}, \quad (4)$$

where $E_0(N_e, N_a)$ is the ground state energy of a system with N_a sites and N_e electrons. Here, the filling n is defined by $n = N_e/N_a$.

We numerically diagonalize the Hamiltonian Eq. (1) up to 20 sites system using the standard Lanczos algorithm. Using the definitions of Eqs. (3) and (4), we calculate D and χ_c from the ground state energy of the finite size system. To carry out a systematic calculation, we use the periodic boundary condition for $N_e = 4m + 2$ and the antiperiodic boundary condition for $N_e = 4m$, where N_e is the total electron number and m is an integer. This choice of the boundary condition removes accidental degeneracy so that the ground state might always be a singlet with zero momentum.

At quarter filling, the $8k_F$ umklapp scattering is crucial to understanding the MIT. The effect of the umklapp term is renormalized under the change of the cutoff $\alpha \rightarrow e^\ell \alpha$. In this work, we adopt the Kehrein's formulation as the RG equations^{16,17}

$$\frac{dK_\rho(\ell)}{d\ell} = -8 \frac{G(\ell)^2 K_\rho(\ell)^2}{\Gamma(8K_\rho(\ell) - 1)}, \quad (5)$$

$$\frac{d \log G(\ell)}{d\ell} = [2 - 8K_\rho(\ell)], \quad (6)$$

where the scaling quantity ℓ is related to the cutoff α , $\Gamma(x)$ is Γ -function and $G(0) = g_{3\perp}/2\pi\alpha^2 v_\rho$. This formulation is an extension of the perturbative RG theory and allows us to estimate the charge gap together with K_ρ in the infinite size system. To solve these equations concretely, we need an initial condition for the two values: $K_\rho(0)$ and $G(0)$. Here, the value of the short-distance cutoff α is selected to a lattice constant of the system and set to be unity. Although the continuum field theory does not give this cutoff parameter, our choice is quite natural to apply this method to the lattice system.

In the weak-coupling limit, analytic expressions for the initial condition have been obtained¹³. At quarter filling, v_ρ , $g_{3\perp}$ and $K_\rho(0)$ are given by $\{(2\pi v_F + U + 4V)^2 - (U + 4V)^2\}^{1/2}/2\pi$, $(U - 4V)U^2/(2\pi v_F)^2$ and $\{1 + (U + 4V)/(\pi v_F)\}^{-1/2}$, respectively, where v_F is $2t \sin k_F$. When we substitute these values into the RG equations as the initial condition, we find the insulating states for $U \gtrsim 8$ at $V = 0$ in contrast to the exact results which show the metallic states for all U at $V = 0$. This inconsistency suggests that the analytical initial condition is not applicable in the strong coupling regime.

To find an adaptable initial condition to the strong coupling regime, we diagonalize a L -site system numerically and calculate $K_\rho(\ell)$ by using the relation $\ell \simeq \ln L$. It is easy for the numerical calculation to obtain $K_\rho(\ell)$ as compared to $G(\ell)$. Therefore, we calculate $K_\rho(\ell_1)$ and $K_\rho(\ell_2)$ with L_1 - and L_2 -site systems instead of $K_\rho(\ell)$ and $G(\ell)$ with a L -site system. To eliminate $G(\ell)$ in the RG equations, we integrate the Eq. (6) and obtain,

$$G(\ell) = G(\ell_0) e^{\int_{\ell_0}^{\ell} [2 - 8K_\rho(\ell')] d\ell'}, \quad (7)$$

where ℓ_0 is a constant. Then the differential equation for $K_\rho(\ell)$ is written by

$$\frac{dK_\rho(\ell)}{d\ell} = -8 \frac{G^2(\ell_0) e^{\int_{\ell_0}^{\ell} [4 - 16K_\rho(\ell')] d\ell'} K_\rho(\ell)^2}{\Gamma(8K_\rho(\ell) - 1)}. \quad (8)$$

When we set $\ell_0 = \ell_1$ and use $K_\rho(\ell_1)$ as the initial condition for the above equation, we can obtain the solution numerically except the constant $G(\ell_1)$. By fitting the value of this solution at $\ell = \ell_2$ to $K_\rho(\ell_2)$, we can determine $G(\ell_1)$. Then, $G(\ell)$ is immediately calculated from Eq. (7) and the solution of the RG equations is completely obtained.

III. DETAILED ANALYSIS OF K_ρ

In Fig. 1, we show the RG flow obtained by solving the RG equations with the numerical and the analytical

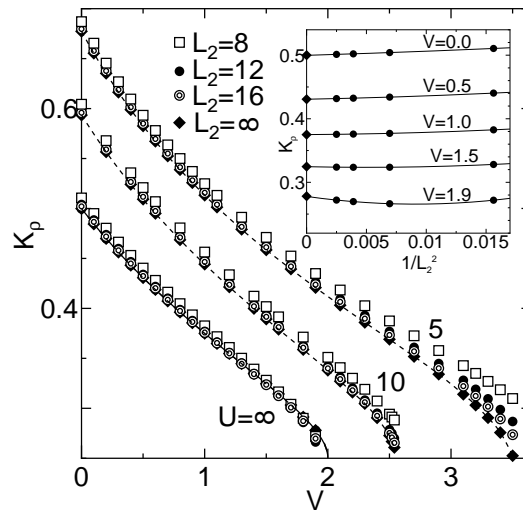


FIG. 2. $K_\rho^{L_2}(\infty)$ as a function of V at $U = 5$ 10 and ∞ with the exact result at $U = \infty$ (the solid line). The broken lines are guides for the eye for the data of $K_\rho^\infty(\infty)$. Inset shows $K_\rho^{L_2}(\infty)$ as a function of $1/L_2^2$ for various V at $U = \infty$ (filled circles) together with the exact result (filled diamonds).

initial conditions on the $K_\rho(\ell)$ - $G(\ell)$ plane. Here, we set $L_1 = 8$ and $L_2 = 12$ for the numerical initial condition. In the weak coupling regime with $U \lesssim 5$, the renormalized $K_\rho(\infty)$ obtained from both the initial conditions agree with the Bethe ansatz result. On the other hand, in the strong coupling regime with $U \gtrsim 5$, there is a large discrepancy between $K_\rho(\infty)$ with the analytical initial condition and the exact result. This is a striking contrast to the numerical initial condition which yields $K_\rho(\infty)$ in excellent agreement with the exact result even in the limit $U \rightarrow \infty$.

In the inset of Fig. 1, we plot the RG flow of $K_\rho(\ell)$ as a function of L^{-1} for various V at $U = \infty$ together with $K_\rho(\ell)$ from the numerical diagonalization for several system sizes L and from the exact results for $L = \infty$. The RG flow seems to connect smoothly the numerical results and the exact result. It indicates that the size dependence of $K_\rho(\ell)$ is well described by the RG equations. For $U = \infty$, our result is consistent with the previous result from Emery and Noguera¹⁸. They solved the RG equations with the numerical initial conditions $K_\rho(\ell)$ and $G(\ell)$ for a system size L , where $G(\ell)$ is calculated from the excited state energy. On the other hand, in our approach, we need only the value of $K_\rho(\ell)$ which is calculated from the ground state. Then, our approach can be easily extended to a complicated model such as the extended Hubbard model with finite U in contrast to the previous approach¹⁸ which has been applied only for the infinite U case.

In order to check the dependence of $K_\rho(\infty)$ on the system sizes L_1 and L_2 for the initial condition, we cal-

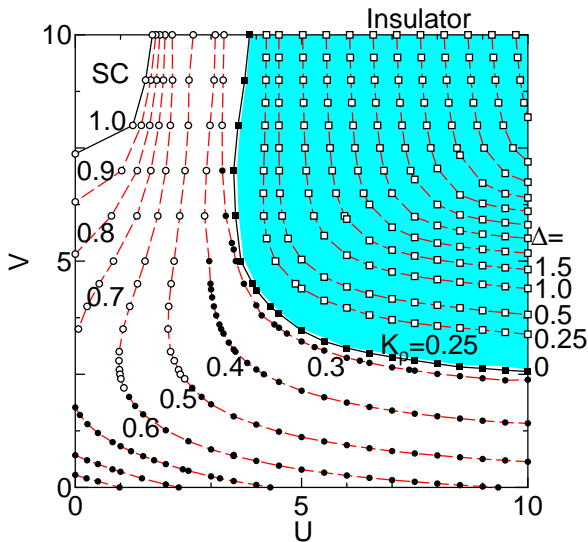


FIG. 3. The contour lines for $K_\rho^\infty(\infty)$ and for the charge gap on the U - V plane. The solid circles are $K_\rho^\infty(\infty)$ from the RG equations with numerical initial conditions, and the open circles are the numerical diagonalization results (see in the text). The open squares represent the charge gap (Ref. 10), whose values are 0.25, 0.5, 1, 1.5, 2, 2.5, 3, 3.5, 4, 4.5, 5 and 5.5. The filled squares represent the phase boundary of the MIT where $K_\rho^\infty(\infty) = 1/4$.

culate $K_\rho(\infty)$ by using the three different sizes $L_2 = 8, 12$ and 16 with $L_1 = L_2 - 4$. In Fig. 2, we show $K_\rho(\infty)$ as a function of V for $U = 5, 10$ and ∞ together with the exact result for $U = \infty$. The value of $K_\rho(\infty)$ is slightly dependent on L_2 . The inset in Fig. 2 shows the L_2 dependence of $K_\rho(\infty)$ for various V at $U = \infty$ together with the corresponding exact result. Here, we assume that the size dependence of $K_\rho(\infty)$ is given by $K_\rho^{L_2}(\infty) \sim K_\rho^\infty(\infty) + c_1/L_2^2 + c_2/L_2^4$, where c_1 and c_2 are constants, and $K_\rho^\infty(\infty)$ is the $L_2 \rightarrow \infty$ extrapolated value of $K_\rho(\infty)$. We see that $K_\rho^\infty(\infty)$ is very close to the exact result for $U = \infty$. We may expect that the RG equations with numerical initial conditions give a reliable estimate for $K_\rho^\infty(\infty)$ not only for the infinite U case but also for the finite U case where the exact result is not known so far.

When the strength of V exceeds a critical value V_c , $K_\rho(\infty)$ is renormalized to the value of the strong coupling limit: $K_\rho = 1/4$. This critical point corresponds to the MIT point of the system. In the infinite U case, we find $V_c \simeq 1.93, 1.95$ and 1.96 for $L_2 = 12, 16$ and 20 , respectively. Assuming the size dependence of V_c to be $\propto 1/L_2^2$, we obtain an $L_2 \rightarrow \infty$ extrapolated value $V_c = 1.99$. It agrees well with the exact value $V_c = 2$ for $U = \infty$. The similar extrapolation yields the critical values of the MIT: $V_c \simeq 3.45$ for $U = 5$ and $V_c \simeq 2.55$ for $U = 10$ as shown in Fig. 2²⁰. The results are in good

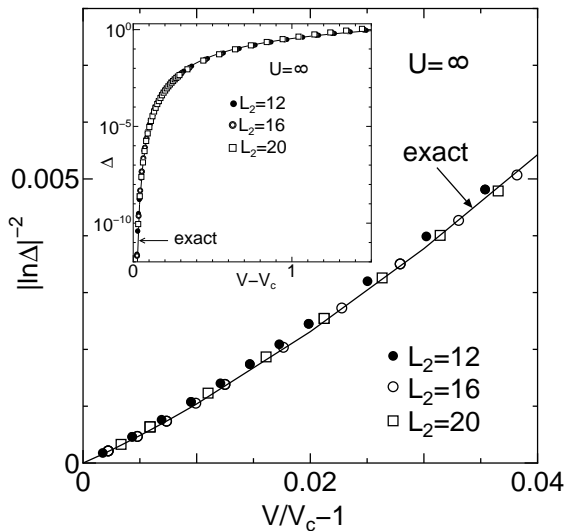


FIG. 4. $|\ln \Delta|^{-2}$ as a function of $(V/V_c - 1)$ near the MIT at $U = \infty$ for $L_2 = 12, 16$ and 20 together with the exact result (solid line). Inset shows Δ as a function of $V - V_c$.

agreement with the phase boundary of the MIT in the previous works⁵⁻¹⁰. Then it confirms that the combined approach of the ED and the RG methods gives accurate results of K_ρ even near the MIT.

In Fig. 3, we show the phase diagram of the MIT on the U - V plane together with the contour lines for $K_\rho^\infty(\infty)$ in the metallic region. We also plotted the contour lines for the charge gap in the insulating region which have already been reported in our previous paper^{10,19}. When $V \gg U$, the SC phase with $K_\rho > 1$ appears. The character of this phase has already been discussed in the previous works⁵⁻⁸. Near the SC phase, $K_\rho(\ell_2)$ is larger than $K_\rho(\ell_1)$ for available finite size systems and, then, we could not obtain the solution of the RG equations for these initial conditions. Because the umklapp scattering is canceled by the SC fluctuation, the RG equations may not be applicable in this region. Thus we estimate K_ρ for $V \gg U$ directly by the ED method without the use of the RG method.

IV. CRITICAL BEHAVIOR NEAR THE MIT

Now we examine the critical behavior of the renormalized K_ρ and the charge gap Δ near the MIT. In the strong coupling region with $K_\rho < 1/4$, the perturbative RG approach leads the running coupling constants $G(\ell)$ and $K_\rho(\ell)$ into divergence. To avoid this difficulty, Kehrein^{16,17} introduced a renormalized coupling constant $\tilde{G}(\ell)$ constructed by the product of $G(\ell)$ and the effective energy scale $e^{-\ell(2-8K_\rho)}$. In the limit $\ell \rightarrow \infty$, $G(\ell)$ diverges in proportional to $e^{\ell(2-8K_\rho)}$ (see Eq. (7)), while

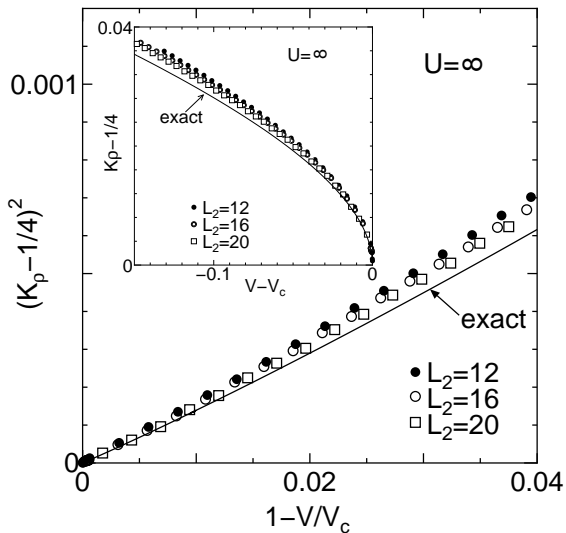


FIG. 5. $(K_\rho - 1/4)^2$ as a function of $(1 - V/V_c)$ near the MIT at $U = \infty$ for $L_2 = 12, 16$ and 20 together with the exact result (solid line). Inset shows $K_\rho - 1/4$ as a function of $V - V_c$.

$\tilde{G}(\ell)$ remains a finite value and is related to the charge gap as

$$\Delta = cv_\rho \tilde{G}(\infty), \quad (9)$$

where c is a factor of the order of unity. Within the RG method, the explicit value of c is not determined. On the other hand, in the combined approach of the ED and the RG methods, we can explicitly determine the factor c by fitting the RG result of Δ to the numerical result from the ED method, which will be done below.

A. V -dependence for $U = \infty$

First, we examine the critical behavior near the MIT for $U = \infty$, where the MIT takes place when V is varied. In this case, we can test the reliability of our approach by comparing with the available exact results. Figure 4 shows the critical behavior of the charge gap Δ calculated from the combined approach of the ED and the RG methods with $L_2 = 12, 16$ and 20 at $U = \infty$, where $|\ln \Delta|^{-2}$ is plotted as a function of $(V/V_c - 1)$ together with the exact result. In the inset in Fig. 4, Δ is plotted as a function of $V - V_c$. Here, the factor c in Eq. (9) is determined by fitting the RG result of Δ to the numerical result from the ED method at $V - V_c = 1$, where the system is away from the critical regime of the MIT and the ED method without the RG method can give an accurate result of Δ .

As shown in Fig. 4, the critical behavior from our approach agrees very well with the exact result which is given by

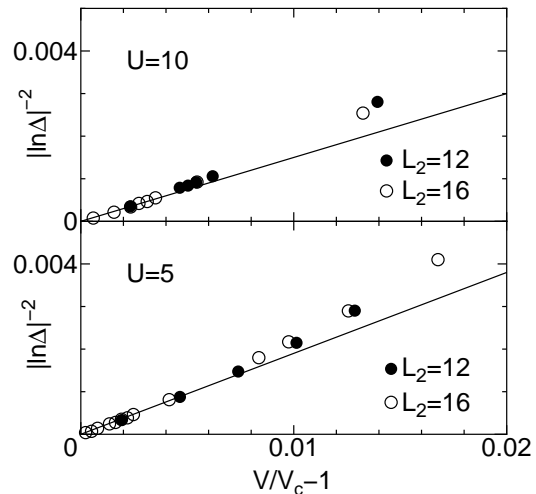


FIG. 6. $|\ln \Delta|^{-2}$ as a function of $(V/V_c - 1)$ near the MIT for $U = 10$ and $U = 5$ with $L_2 = 12$ and 16 together with the straight lines whose slope are 0.20 for $U = 10$ and 0.22 for $U = 5$. Here, the factor of Δ is determined by fitting Δ to the numerical result at $V - V_c = 1$.

$$\frac{1}{|\ln \Delta|^2} = c_\Delta \left(\frac{V}{V_c} - 1 \right), \quad (10)$$

for $0 < (V/V_c - 1) \ll 1$, where $c_\Delta = \frac{8}{\pi^4}^{14}$. From the results shown in Fig. 4, we estimate the coefficient as $c_\Delta \sim 0.087, 0.084$ and 0.082 for $L_2 = 12, 16$ and 20 , respectively. Assuming the size dependence as $\propto 1/L_2^2$, we obtain an $L_2 \rightarrow \infty$ extrapolated value $c_\Delta \sim 0.080$ which is close to the exact result of $c_\Delta = \frac{8}{\pi^4} \simeq 0.0821$. Thus, our approach gives reliable estimates for the charge gap Δ with very small energy scale near the MIT. It is noted that the perturbative RG approach also yields the same critical behavior given in Eq. (10) but fails to determine the explicit value of the coefficient c_Δ ^{8,21}.

As for the critical behavior of K_ρ near the MIT, the perturbative RG approach predicts that $(K_\rho - 1/4)^2 \propto (V_c - V)$, but the coefficient of $(V_c - V)$ is not determined within the approach^{21,22}. In contrast to the perturbative RG method, our combined approach of the ED and the RG methods enables us to estimate the coefficient explicitly. Fig. 5 shows $(K_\rho - 1/4)^2$ as a function of $(1 - V/V_c)$ at $U = \infty$ calculated from our approach together with the exact result. In the critical regime, our result agrees very well with the exact result which is given by

$$\left(K_\rho - \frac{1}{4} \right)^2 = c_K \left(1 - \frac{V}{V_c} \right), \quad (11)$$

for $0 < (1 - V/V_c) \ll 1$, where $c_K = \frac{1}{8\pi^2}$. From the results shown in Fig. 5, we estimate the coefficient as $c_K \sim 0.016, 0.015$ and 0.014 for $L_2 = 12, 16$ and 20 , respectively. Using $1/L_2^2$ extrapolation, we obtain the coefficient in $L_2 \rightarrow \infty$ as $c_K \sim 0.013$ which is again close

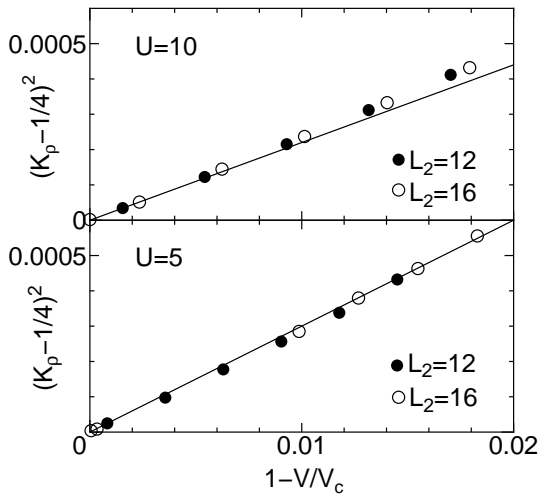


FIG. 7. $(K_\rho - 1/4)^2$ as a function of $(1 - V/V_c)$ near the MIT at $U = 10$ and $U = 5$ for $L_2 = 12$ and 16 together with the straight lines whose slope are 0.019 at $U = 10$ and 0.032 at $U = 5$.

to the exact result $c_K = \frac{1}{8\pi^2} \simeq 0.0127$. This indicates that our approach gives an accurate estimate for K_ρ as well as for Δ even near the MIT beyond the usual finite size scaling for the numerical diagonalization method.

B. V -dependence for finite U

Next, we examine the critical behavior of Δ and K_ρ in the finite U case. In this case, there is no available exact result. In Fig. 6, we plot $|\ln \Delta|^{-2}$ as a function of $(V/V_c - 1)$ near the MIT for $U = 10$ and 5 . We find that the critical behavior for both $U = 10$ and 5 is the same as that for $U = \infty$ given in Eq. (10) except the value of the coefficient c_Δ . For $U = 10$, we estimate the coefficient as $c_\Delta \sim 0.15$ and 0.15 for $L_2 = 12$ and 16 , respectively, which yield an $L_2 \rightarrow \infty$ extrapolated value $c_\Delta \sim 0.15$. For $U = 5$, the values of the coefficient are $c_\Delta \sim 0.17$ and 0.18 for $L_2=12$ and 16 , respectively, resulting in an $L_2 \rightarrow \infty$ extrapolated value $c_\Delta \sim 0.19$.

Fig. 7 shows the critical behavior of K_ρ for $U = 10$ and $U = 5$. We again find that the critical behavior for both $U = 10$ and 5 is the same as that for $U = \infty$ given in Eq. (11) except the value of the coefficient c_K . We estimate the values of c_K for $U = 10$ as $c_K \sim 0.022$ and 0.022 for $L_2=12$ and 16 , respectively. For $U = 5$, the values of the coefficient are 0.028 and 0.029 for $L_2=12$ and 16 , respectively. These results yield $L_2 \rightarrow \infty$ extrapolated values $c_K \sim 0.022$ for $U = 10$ and $c_K \sim 0.030$ for $U = 5$.

When U decreases from $U = \infty$, both c_Δ and c_K monotonically increase and become considerably large for a suitable value of U such as $U = 10$ and 5 as compared to the corresponding values of c_Δ and c_K for $U = \infty$.

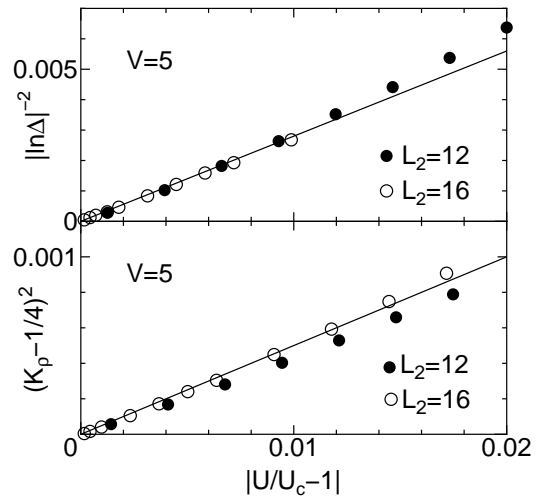


FIG. 8. $(K_\rho - 1/4)^2$ as a function of $(1 - V/V_c)$ near the MIT at $U = 10$ and $U = 5$ for $L_2 = 12$ and 16 together with the straight lines whose slope are 0.019 at $U = 10$ and 0.032 at $U = 5$.

C. U -dependence for finite V

In the large V regime ($V > U$), the MIT takes place at a critical value U_c when U is varied for a fixed value of V as found in Fig. 3. Finally, we examine the critical behavior in this case. In Fig. 8, $|\ln \Delta|^{-2}$ and $(K_\rho - 1/4)^2$ are plotted as functions of $|U/U_c - 1|$ near the MIT for $V = 5$. We find that the critical properties as functions of U/U_c are the same as those as functions of V/V_c given in eqs. (10) and (11) except the values of the coefficients: $|\ln \Delta|^{-2} = c'_\Delta (U/U_c - 1)$ and $(K_\rho - \frac{1}{4})^2 = c'_K (1 - U/U_c)$ in the limit $U \rightarrow U_c$, respectively. We estimate the coefficients as $c'_\Delta \sim 0.28$ and $c'_K \sim 0.041$ for $L_2 = 12$ and $c'_\Delta \sim 0.28$ and $c'_K \sim 0.046$ for $L_2 = 16$, which yield $L_2 \rightarrow \infty$ extrapolated values as $c'_\Delta \sim 0.28$ and $c'_K \sim 0.050$, respectively. Both of c'_Δ and c'_K are considerably larger than the corresponding values of c_Δ and c_K .

V. SUMMARY AND DISCUSSION

In summary, we studied the critical behavior near the MIT in the one-dimensional extended Hubbard model at quarter filling by using the combined approach of the ED and the RG methods. In the large U regime ($U > V$), the MIT takes place at a critical value V_c when V is varied for a fixed U , while, in the large V regime ($V > U$), it takes place at a critical value U_c when U is varied for a fixed V . We examined the critical behavior near the MIT for both cases.

In the large U regime, we observed the critical behavior, $|\ln \Delta|^{-2} = c_\Delta (V/V_c - 1)$ and $(K_\rho - \frac{1}{4})^2 =$

$c_K(1 - V/V_c)$, where the critical value V_c and the coefficients c_Δ and c_K are functions of U . For $U = \infty$, the estimated values of V_c , c_Δ and c_K agree well with the exact results. When U decreases from $U = \infty$, all of V_c , c_Δ and c_K monotonically increase. Both of c_Δ and c_K become considerably large for a suitable value of U such as $U = 10$ and 5 as compared to the corresponding values of c_Δ and c_K for $U = \infty$.

In the large V regime, we also observed the same critical properties, $|\ln \Delta|^{-2} = c'_\Delta(U/U_c - 1)$ and $(K_\rho - \frac{1}{4})^2 = c'_K(1 - U/U_c)$. Both of c'_Δ and c'_K are considerably larger than the corresponding values of c_Δ and c_K . For $V \gg U$, the SC phase with $K_\rho > 1$ appears. Near the SC phase, it is difficult to obtain the solution for the RG equation, because the umklapp scattering is canceled by the SC fluctuation. To examine the critical behavior near the MIT for $V \gg U$, we need an improved RG approach which includes both effects of the umklapp scattering and the SC fluctuation.

We also obtained the phase diagram on the $U - V$ plane and found that the phase boundary of the MIT and the contour lines of Δ and K_ρ near the MIT smoothly connect between the large U regime and the large V regime. Although it is difficult to analyze the critical behavior for $V \gg U$, there is no qualitative difference in the critical behavior. These results suggest that the nature of the MIT is essentially unchanged on the $U - V$ plane over the whole parameter regime including the large U and the large V regimes.

In the limit $V = \infty$, electrons are completely inhibited to occupy the nearest neighbor site of each other. In this case, some exact results have been obtained in the previous works⁵⁻⁸: the ground state energy is always zero for $U > U_c (= 4)$ and the charge gap is given by $\Delta = |U - U_c|$. Then, the critical behavior of Δ for $V = \infty$ is completely different from that for finite V case obtained here. We think that there are two possibilities to explain this differences as follows: (1) The critical behavior near the MIT changes discontinuously at a finite V . (2) The critical region smoothly shrinks with increasing V and finally becomes zero in the limit $V = \infty$ where the different critical behavior is observed. In any case, the critical behavior near the MIT for $V \gg U$ is interesting problem as the competition between the SC fluctuation and the umklapp scattering becomes important, and will be studied in the future.

- ⁵ F. Mila and X. Zotos, Europhys. Lett. **24**, 133 (1993).
- ⁶ K. Sano and Y. Ōno, J. Phys. Soc. Jpn. **63**, 1250 (1994).
- ⁷ K. Penc and F. Mila, Phys. Rev. B **49**, 9670 (1994).
- ⁸ M. Nakamura, Phys. Rev. B **61**, 16377 (2000). He shows the phase boundary of the MIT by observing the level crossing of the excitation spectra of finite size systems.
- ⁹ K. Sano and Y. Ōno, J. Phys. Chem. Solids. **62**, 281 (2001).
- ¹⁰ K. Sano and Y. Ōno, J. Phys. Chem. Solids. **63**, 1567 (2002).
- ¹¹ Y. Shibata, S. Nishimoto and Y. Ohta: Phys. Rev. **B64**, 513 (2002).
- ¹² M. Tsuchiizu, H. Yoshioka and Y. Suzumura, Physica **B284-288**, 1547 (2000).
- ¹³ H. Yoshioka, M. Tsuchiizu and Y. Suzumura, J. Phys. Soc. Jpn. **69**, 651 (2000).
- ¹⁴ C. N. Yang and C. P. Yang, Phys. Rev. **151**, 258 (1966).
- ¹⁵ A. Luther and Peschel, Phys. Rev. B **9**, 2911 (1974).
- ¹⁶ S. Kehrein, Phys. Rev. Lett. **83**, 4914 (1999).
- ¹⁷ S. Kehrein, Nucl. Phys. **B592**, 512 (2001).
- ¹⁸ V. J. Emery and C. Noguera, Phys. Rev. Lett. **60** (1988) 631; They evaluated the umklapp scattering G by the level splitting of a finite size system and calculated the Luttinger-liquid parameter K_ρ from the RG equations in the limit $U \rightarrow \infty$.
- ¹⁹ The charge gap is determined by $E(L/2+1) + E(L/2-1) - 2E(L/2)$, where $E(L/2)$ is the total energy of the ground state for a system with $L/2$ electrons and is calculated up to 16 sites systems. The size dependence of $\Delta(L)$ is assumed as $\Delta(L) = \Delta(\infty) + c_1/L + c_2/L^2$, where c_1 and c_2 are constants.
- ²⁰ In the case of $U = 10$, we estimate $V_c \simeq 2.58$ and 2.57 for $L_2 = 12$ and 16 , respectively. For $U = 5$, $V_c \simeq 3.65$ and 3.57 for $L_2 = 12$ and 16 , respectively.
- ²¹ J. M. Kosterlitz, J. Phys. **C7**, 1046 (1974).
- ²² The critical behavior of K_ρ is determined by the deviation from the critical line at $\ell \rightarrow \infty$.

¹ V. J. Emery, in *Highly Conducting One-Dimensional Solids*, edited by J. T. Devreese, R. Evrand and V. van Doren, (Plenum, New York, 1979), p.327.

² J. Sólyom, Adv. Phys. **28**, 201 (1979).

³ J. Voit: Rep. Prog. Phys. **58**, 977 (1995).

⁴ H. Q. Lin and J. E. Hirsch, Phys. Rev **B33**, 8155 (1985).